Electronic Supplementary Material (ESI) for Physical Chemistry Chemical Physics.
This journal is © the Owner Societies 2023

Supplementary Material: Controlling Surface Cation Segregation in a Double Perovskite for Oxygen Reduction, Evolution, and Transport in Energy Storage Devices.

Jyotsana Kala,[†] Uzma Anjum,[‡] Brajesh Kumar Mani,[*,†] and M. Ali Haider[*,‡]

†*Department of Physics, Indian Institute of Technology Delhi, Hauz Khas, New Delhi-110016, Delhi, India*

‡*Department of Chemical Engineering, Indian Institute of Technology Delhi, Hauz Khas, New Delhi-110016, Delhi, India*

E-mail: Brajesh.Kumar.Mani@physics.iitd.ac.in; haider@iitd.ac.in

Calculation of U values for Nd and Co atoms in $NdBaCo_2O_{5+\delta}$

In order to accurately describe the strongly correlated d and f -electrons of Co and Nd, respectively, we incorporated the U correction in the DFT calculations. The hubbard U parameter is extracted from data on electron occupancy as function of applied perturbation self-consistently using Cococcioni approach. Figs. 1 and 2 shows the calculation of U values for Co and Nd, respectively. The values estimated are 3.37 eV and 6.01 eV for d and f -electrons of Co and Nd, respectively.

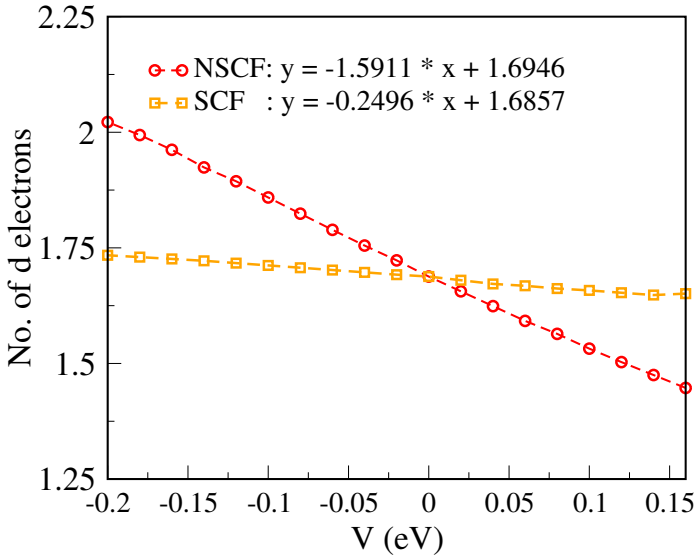

Figure 1: Calculation of U value calculation for Co

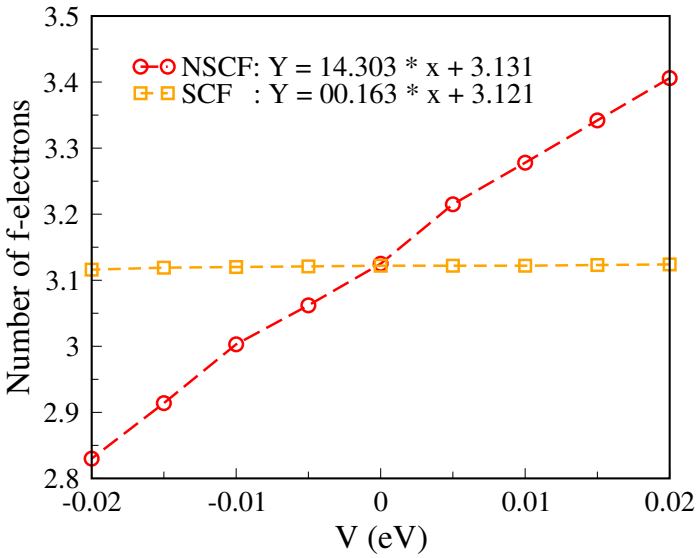

Figure 2: Calculation of U value calculation for Nd

Radial pair distribution function plots for Co/Ba and Ba/Co surface slabs of $NdBaCo_2O_6$

For more information of the Ba cation disorder at the Co/Ba surface. the radial distribution functions (RDF) of Ba^{+2}-Ba^{-2} and Ba^{+2}-O^{-2} are plotted with respect to interatomic

distances. The more diffused curves at distances greater than nearest neighboring distance predicts more cation movement and hence Ba cation segregation.

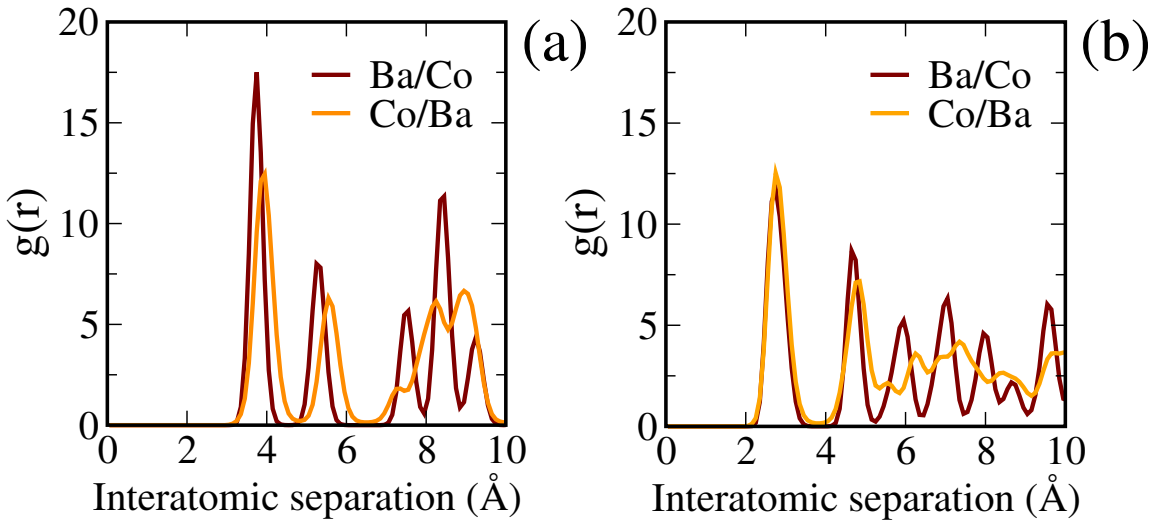

Figure 3: Radial distribution function (g(r)) plotted for (a) Ba^{+2}-Ba^{-2}, and (b) Ba^{+2}-O^{-2} pairs with respect to interatomic distances

Electronic structures of unstrained and strained NBCO

The density of states plots are obtained are for unstrained and 4% tensile strained NBCO, Fig. 4. As we observed from the figure, the asymmetry in the spin-up and down channels has increased n the case of 4% tensile strained NBCO. Examining the partial density of states more closely, we find that the f -electrons of Nd atom contribute more dominantly to this spin asymmetry, leading to an increased magnetic moment.

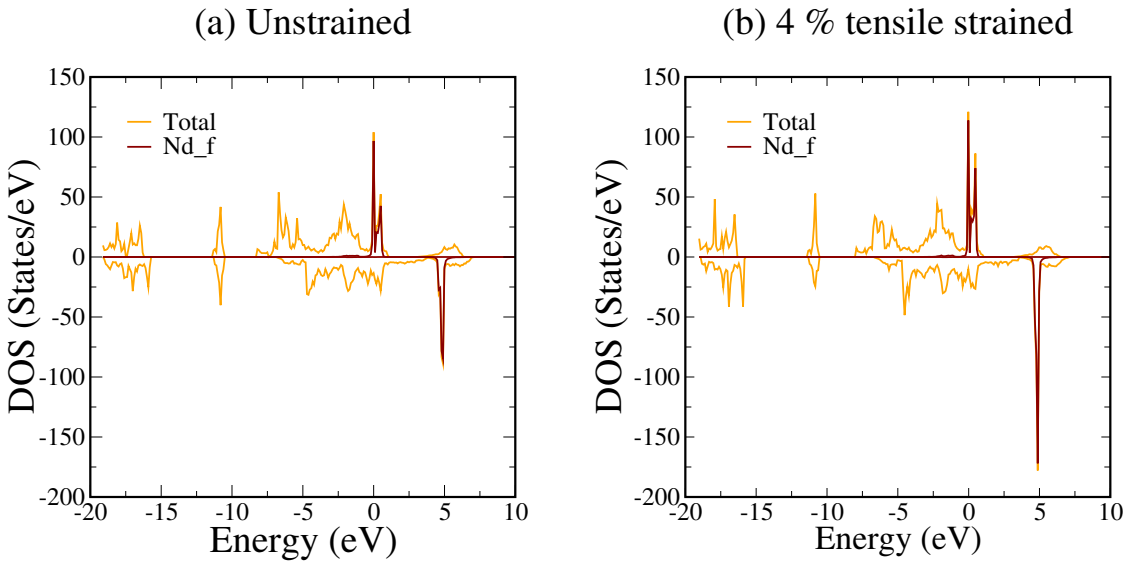

Figure 4: Density of states for (a) unstrained, and (b) 4 % tensile strained NBCO

Oxygen density profile and radial distribution function plots for 4 % tensile strained NBCO

In order to understand the effect of lattice strain on oxygen anion diffusivity, ionsâĂŹ dynamics is traced for 1 ns using MD simulations. Fig. 4 shows the oxygen anion density profile for 4% tensile strained NBCO. As discernible from the figure, we observed an increased oxygen anion diffusivity. Fig. 5(b) represents the radial pair distribution functions plotted for O^{-2}-O^{-2} pair in unstrained and 4 % tensile strained NBCO. As obtained from Fig. 5(b), the oxygen anion will be more diffused in 4 % tensile strained NBCO as compared to unstrained NBCO.

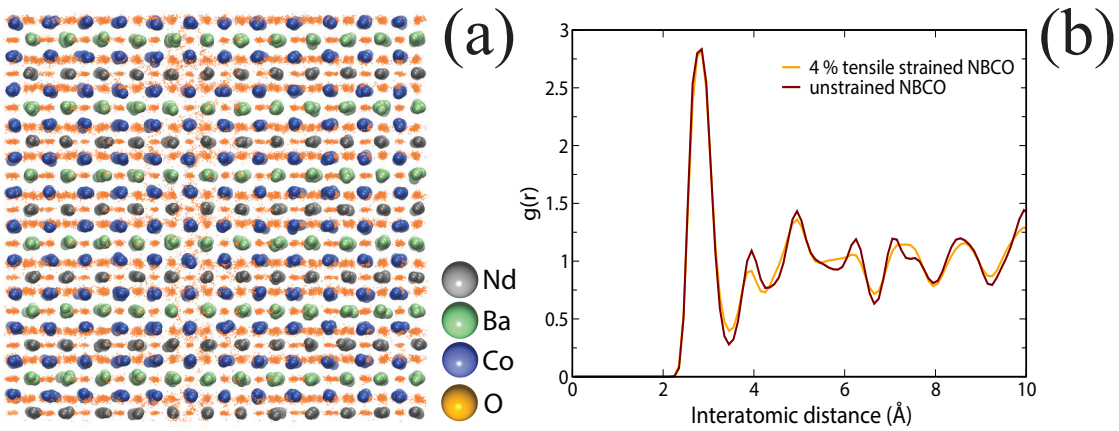

Figure 5: (a) Oxygen anion density profile, visualized after 1 ns of 4 % tensile strained NBCO at 973 K, (b) Radial pair distribution functions plotted for O^{-2}-O^{-2} pair in unstrained and 4 % tensile strained NBCO

Sr-doped oxygen vacancy and surface energy strctures

The following figure represents the oxygen vacancy and surface energy calculations structures for 50 % Sr doped NBCO.

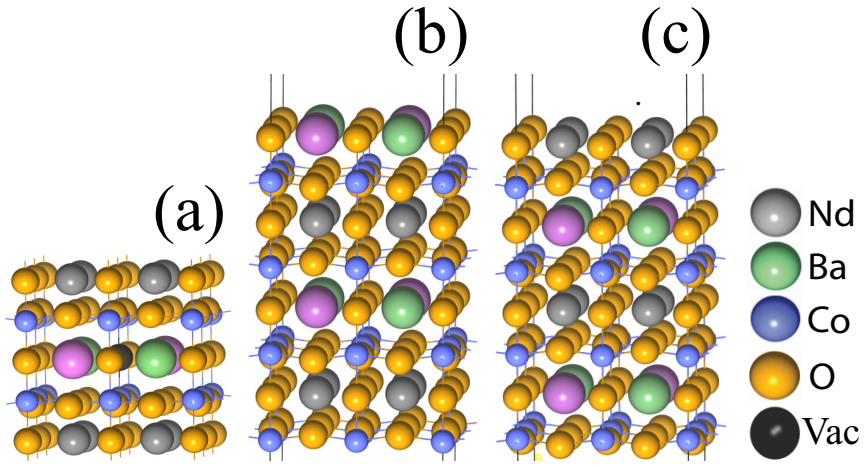

Figure 6: (a) $NdBa_{0.5}Sr_{0.5}Co_2O_{5+\delta}$ with oxygen vacancy in $Ba_{0.5}Sr_{0.5}$/O plane and surface slabs with (b) $Ba_{0.5}Sr_{0.5}$/Co and (c) Nd/Co terminations

Radial distribution function plots for O^{-2}-O^{-2} pairs in NBCO and 50NBSCO

Following figure shows the radial pair distribution functions for O^{-2}-O^{-2} pairs in NBCO and 50NBSCO. As decernible from the structure, the oxygen anion diffusion is higher in 50NBSCO as compared to NBCO.

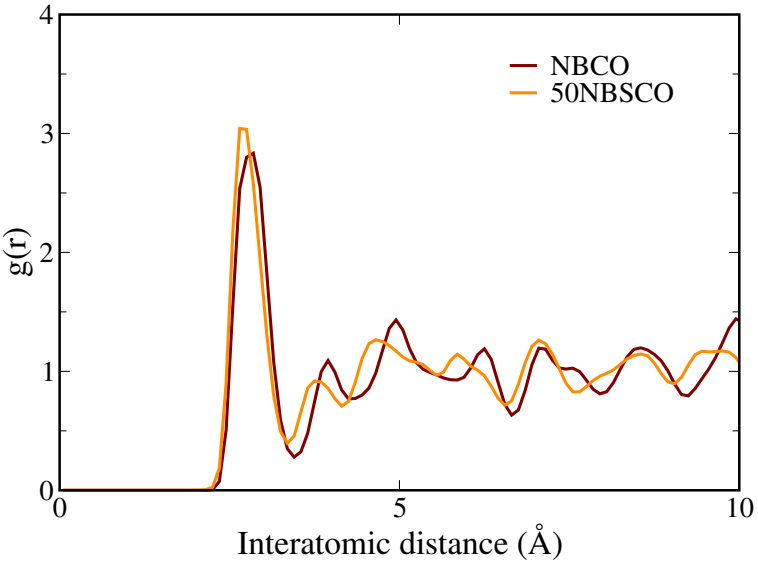

Figure 7: Radial pair distribution functions plotted for O^{-2}-O^{-2} pair in NBCO and 50NBSCO

Segregation energy structures for cation on surface and in bulk of $NdBa_xSr_{1-x}Co_2O_6$ and $NdBa_xCa_{1-x}Co_2O_6$

Segregation energy is obtained as the difference of the DFT energies of the two structures, one when the cation is present on the surface (Cat/Surf) and other when the cation is present in the bulk (Cat/Bulk). Fig. 5 shows the corresponding structures for the calculations of segregation energies, which are used to estimate the Ba, Sr and Ca segregation in doped NBCO.

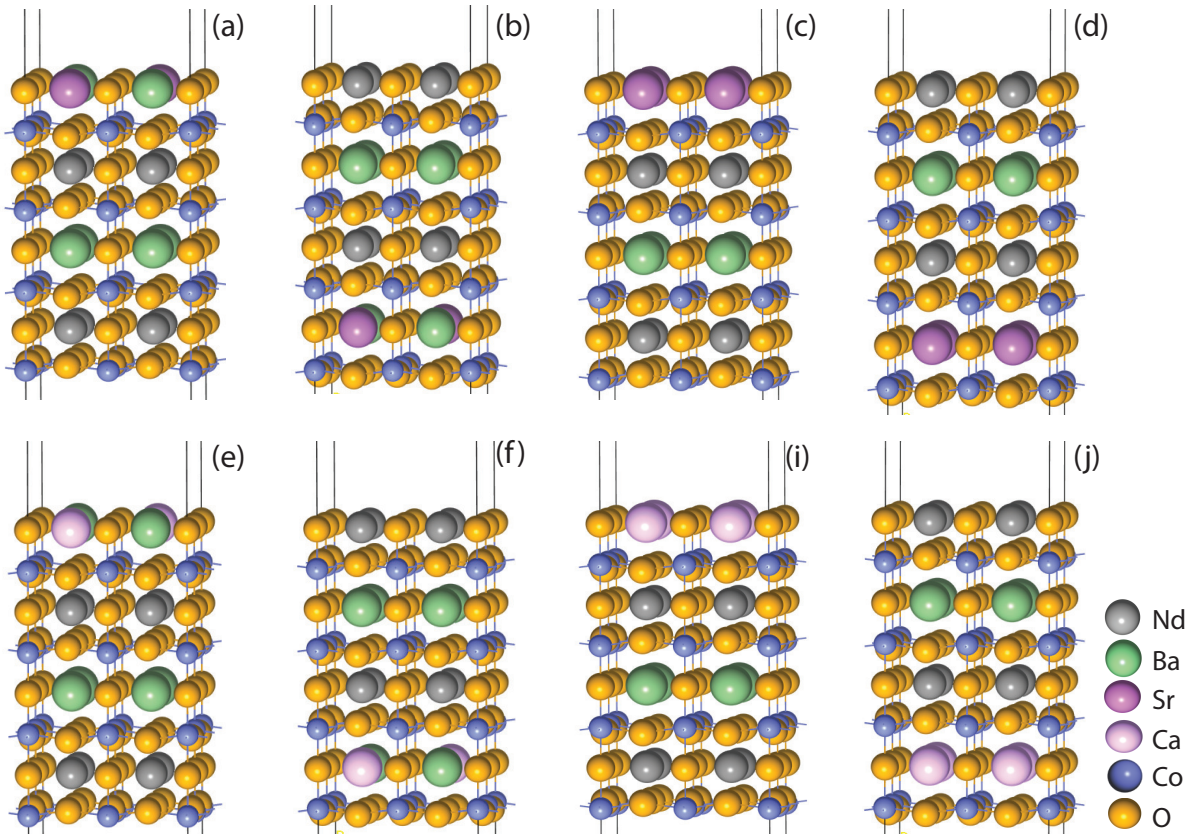

Figure 8: Segregation energy structures with cation on surface and bulk, (a), (c) (Sr,Surf), and (b), (d) (Sr,Bulk) for $NdBa_{0.75}Sr_{0.25}Co_2O_6$ and $NdBa_{0.5}Sr_{0.5}Co_2O_6$, (e), (i) (Ca,Surf), and (f), (j) (Ca,Bulk) for $NdBa_{0.75}Ca_{0.25}Co_2O_6$ and $NdBa_{0.5}Ca_{0.5}Co_2O_6$

Radial distribution function plots for Ba^{-2}-O^{-2}, Sr^{-2}-O^{-2}, and Ca^{-2}-O^{-2} pairs in 25NBSCO and 50NBCCO

Following figure shows the radial pair distribution functions for Ba^{-2}-O^{-2}, Sr^{-2}-O^{-2}, and Ca^{-2}-O^{-2} pairs in 25NBSCO and 50NBCCO. As decernible from the structure, the cation disorder is much higher in 25NBSCO as compared to 50NBCCO.

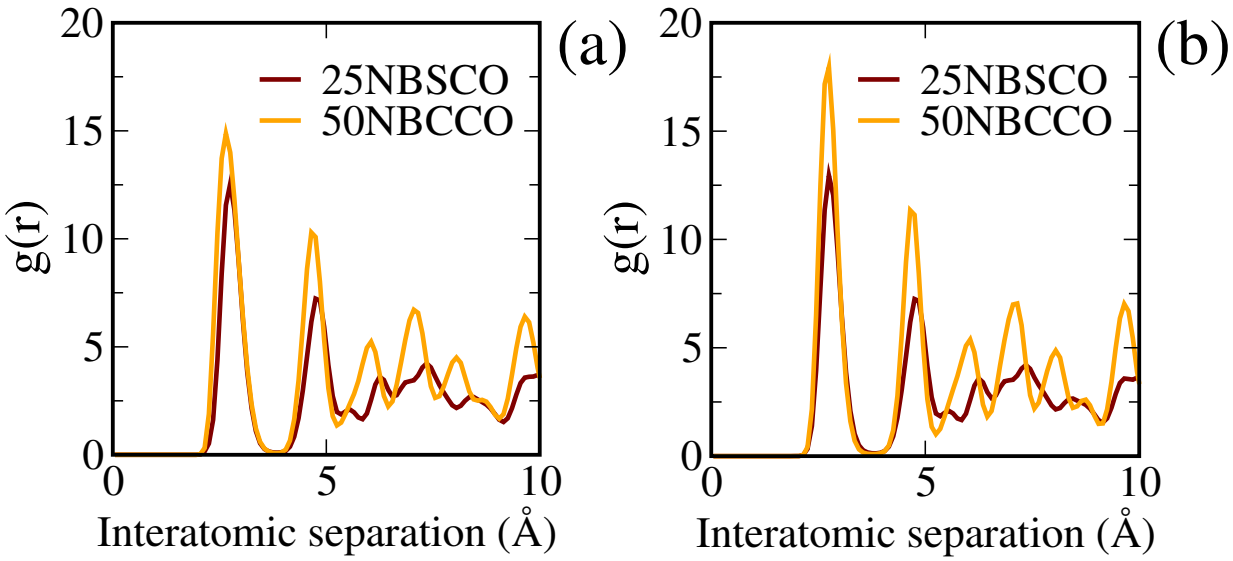

Figure 9: Radial pair distribution functions plot with respect to interatomic distance for (a) Sr^{-2}-O^{-2} in 25NBSCO and Ca^{-2}-O^{-2} in 50NBCCO, and (b)Ba^{-2}-Ba^{-2}in both 25NBSCO and 50NBCCO

Bader Charges

The average charges associated with Nd, Co and Ba cations for $\delta = 1$ and 0.5 is shown in the Table 1. As evident from the table, we observe a charge redistribution on the formation of oxygen vacancies in the structure.

Table 1: Bader charges on Nd, Ba, and Co cation in $NdBaCo_2O_{5+\delta}$

δ	Nd cations	Co cations	Ba cations
0	2.15	1.42	1.56
0.5	2.07	1.35	1.57

Oxygen anion diffusivity in bulk $NdBaCoO_{5.5}$ with temperature

From our simulations we found the oxygen anion diffusivity to be thermally active. In Table 2 we have provided the oxygen anion diffusivity as function of temperature. As evident from the table, the oxygen anion diffusivity is observed to be increasing with increasing temperatures.

Table 2: Oxygen anion diffusivity, estimated for 1 ns of dynamics of ions in bulk $NdBaCo_2O_{5.5}$ with temperature

Temperature (K)	Oxygen Anion Diffusivity ($\times 10^{-7}$ cm^2sec^{-1}
773	1.21 ± 0.23
873	1.76 ± 0.12
973	3.96 ± 0.31
1073	5.52 ± 0.32
1173	8.77 ± 0.14
1273	11.97 ± 0.26

Oxygen anion diffusivity of bulk $NdBaCoO_{5.5}$ with tensile and compressive strain

Lattice strain is reported to change the electrocatalytic properties in SOFC materials. In order to understand the effect of lattice strain on oxygen anion diffusivity, using the MSD vs time data, we extracted the oxygen anion diffusivity for 4% and 2% compressive and tensile strains. The values of oxygen anion diffusivity, at different strains, is given in the Table 3. The oxygen anion diffusivity is observed to increase with increasing tensile strain and decrease with increasing compressive strain.

Table 3: Oxygen anion diffusivity in bulk $NdBaCo_2O_{5.5}$ at 973 K temperature with tensile and compressive strain

Strain (%)	Oxygen Anion Diffusivity ($\times 10^{-7}$ cm^2sec^{-1}
-4	1.11 ± 0.13
-2	2.68 ± 0.25
0	3.96 ± 0.31
2	9.60 ± 0.24
4	10.12 ± 0.43

Oxygen anion diffusivity of bulk $NdBa_xSr_{1-x}CoO_{5.5}$

In order to understand the effect of Sr-doping on electrocatalytic properties, the oxygen anion diffusivity of undoped and doped structure is computed. The data from this is given

in the Table 4. The diffusivity is observed to increase with increasing the Sr content.

Table 4: Oxygen anion diffusivity in Sr-doped bulk $NdBaCo_2O_{5.5}$ at 973 K

Strain (%)	Oxygen Anion Diffusivity ($\times 10^{-7}$ cm^2sec^{-1}
0	3.96 ± 0.31
0.25	5.18 ± 0.26
0.50	8.56 ± 0.42